

**GLYCOLIPID ACQUISITION BY HUMAN GLYCOLIPID TRANSFER PROTEIN
DRAMATICALLY ALTERS INTRINSIC TRYPTOPHAN FLUORESCENCE:
INSIGHTS INTO GLYCOLIPID BINDING AFFINITY***

Xiuhong Zhai¹, Margarita L. Malakhova¹, Helen M. Pike¹, Linda M. Benson², H. Robert Bergen, III², István P. Sugár³, Lucy Malinina⁴, Dinshaw J. Patel⁵, Rhoderick E. Brown¹

¹The Hormel Institute, University of Minnesota, 801 16th Avenue NE, Austin, MN, USA;

²Mayo Proteomics Research Center, Mayo Clinic College of Medicine, Rochester, MN, USA;

³Department of Neurology, Mount Sinai School of Medicine, New York, NY, USA;

⁴Structural Biology, CIC BioGUNE, Parque Tecnológico de Vizcaya, Ed. 800, Derio 48160, Spain;

⁵Structural Biology Program, Memorial Sloan-Kettering Cancer Center, New York, NY, USA;

Running Title: Glycolipid Binding Alters GLTP Tryptophan Emission

Correspondence & reprint requests to: lucy@cicbiogune.es; patel@mskcc.org or reb@umn.edu

Supplementary Information

Incremental lipid presentation via ethanol microinjection enabled rapid ‘solubilization’ by GLTP and minimized light scattering interference so long as glycolipid concentrations were kept low, i.e. each lipid aliquot (2 μ l) representing \sim 10 mole% of total protein (1 μ M; 2.5 ml). As GLTP became saturated and no longer able to ‘solubilize’ the lipid aliquots, the emission response grew moderately noisier, presumably due to light scattering by increasing concentrations of insoluble lipid aggregates and accounting for the less than ideal response expected for a soluble protein interacting with a soluble ligand.

Glycolipids were assumed to occupy a single binding site on GLTP, as indicated by our x-ray structural analyses of human GLTP complexed with different glycolipids (12,13). Because glycolipid binding to GLTP causes a dramatic λ_{max} blue shift (348 to \sim 336 nm), intensities at 353 nm were used for binding isotherms to avoid problems discussed by White and colleagues (31).

The fraction of binding sites (α) occupied by glycolipids was calculated by Equation 1 (59, 60):

$$\alpha = (F - F_0)/F_{\text{max}} \quad (\text{Eq. 1})$$

where F_0 and F are the Trp emission intensities of GLTP in the absence and presence of glycolipid, respectively, and F_{max} is the emission intensity of the fully liganded GLTP, i.e. at excess glycolipid. F_{max} was determined by plotting $1/(F-F_0)$ vs. $1/L$ and extrapolating $1/L = 0$, where L equals the total glycolipid concentration. ΔF_m (maximum fluorescence change when the protein is completely saturated with glycolipid) was determined by plotting $1/L$ (glycolipid concentration) and $1/\Delta F$ (decrease in fluorescence intensity). The concentration of bound glycolipid was calculated using the relationship:

$$[\text{Bound ligand}] = -\text{protein concentration} \times \Delta F/\Delta F_m$$

The free glycolipid concentration was calculated as:

$$[\text{Free glycolipid}] = [\text{Total glycolipid}] - [\text{Bound glycolipid}]$$

Kd values shown in Table 1 were determined by nonlinear curve fitting analyses using Prism 4.0 (GraphPad Software, La Jolla CA). The analysis involved nonlinear regression of a hyperbolic function fit to the saturation isotherm and avoided errors associated with linear transformations, i.e. Scatchard analysis. Binding isotherms shown in Figures 2, 4, and 5 were adjusted for the constant fractional contributions of Trp85 and Trp142 from the emission response of W96F-GLTP.

Glycolipid synthesis and purification. Briefly, the *N*-hydroxy succinimide ester of the fatty acid was prepared, recrystallized and reacted with lyso-sphingolipid (24,25). Reacylation for 6-8 h at 60 °C under nitrogen and in the presence of *N*-ethyl-diisopropylamine catalyst yielded *N*-dodecanoyl LacSph (12:0 LacCer), *N*-hexadecanoyl LacSph (16:0 LacCer), *N*-cis-9-octadecenoyl LacSph, (18:1 ^{Δ 9cis} LacCer or *N*-oleoyl LacCer), *N*-cis-15-tetracosenoyl GalSph (24:1 ^{Δ 15cis} GalCer or *N*-nervonoyl GalCer), *N*-cis-*N*-cis-9,12-octadecenoyl GalSph (18:2 ^{Δ 9,12cis} GalCer or *N*-linoleoyl GalCer), *N*-hexadecanoyl GalSph (16:0 GalCer), *N*-dodecanoyl SPC (12:0 SM), *N*-cis-9-octadecenoyl dodecanoyl SPC (18:1 ^{Δ 9cis} SM), *N*-cis-15-tetracosenoyl SPC (24:1 ^{Δ 15cis} SM or *N*-nervonoyl SM). The resulting sphingolipid was purified by flash column chromatography, crystallized from CHCl₃/CH₃OH using -20°C acetone and analyzed for purity by thin layer chromatography. Acyl homogeneity was confirmed by via capillary gas chromatography after quantitative release and methylation of fatty acyl residues.

D-galactosyl- β 1-1'-*D*-erythroSphingosine (lysoGalCer), D-lactosyl- β 1-1'-*D*-erythroSphingosine (lysoLacCer), D-glucosyl- β 1-1'-*D*-erythroSphingosine (lysoGlcCer), *D*-erythro-Sphingosine phosphocholine (lysoSM), *N*-octanoyl LacSph (8:0 LacCer), *N*-octanoyl GalSph (8:0 GalCer), *N*-octanoyl GlcSph (8:0 GlcCer), *N*-dodecanoyl GlcSph (12:0 GlcCer), *N*-oleoyl GlcSph (18:1 GlcCer), ganglioside GM1,

1-palmitoyl-2-oleyl-*sn*-glycero-3-phosphocholine (POPC), 1,2-dimyristoyl-*sn*-glycero-3-phosphocholine (DMPC), 1-myristoyl-2-palmitoyl-*sn*-glycero-3-phosphocholine (MPPC), 1-myristoyl-2-stearoyl-*sn*-glycero-3-phosphocholine (MSPC) were purchase from Avanti Polar Lipids (Alabaster AL)

Glycolipid intervesicular transfer activity. A fluorescence-based resonance energy transfer (RET) assay involving anthrylvinyl (AV) labeled glycolipid (1 mol%) and a nontransferable perylenoyl-labeled PC (1mol%) permitted continuous real time monitoring of GLTP activity (54). Excitation and emission wavelengths were 370 nm and 425 nm, respectively. POPC donor vesicles containing the fluorescent lipids were prepared by rapid ethanol injection, and POPC acceptor vesicles were prepared by sonication. Initial transfer velocities and other details of this well established assay and are presented elsewhere (34,54-56). RET assay results were corroborated by radiolabeled lipid intervesicular transfer assays. Donor POPC vesicles containing 2 mol% [³H]GalCer, 10 mol% negatively charged dipalmitoyl phosphatidic acid, and a trace of [¹⁴C]tripalmitate (nonexchangeable marker) were prepared by sonication in 10 mM sodium phosphate (pH 7.4), 1 mM DTT, 1 mM EDTA, and 0.02% NaN₃. POPC SUVs prepared similarly, but at 10-20 mM concentration, served as acceptor vesicles. After incubation with GLTP (0.1-1.0 µg), charged donor and neutral acceptor vesicles were separated by rapid elution over DEAE Sephacel minicolumns (27,56). Calculation of glycolipid transfer to the acceptor vesicles and associated rates was analyzed by fitting to first order exponential behavior using OriginPro 7.5 (Northampton, MA).

Preparation of small unilamellar vesicles. Sonicated vesicles (SUVs) were prepared using a slightly modified procedure of Huang and Thompson (57). Briefly, lipid films were obtained by rotary evaporation of the desired lipid mixture in solvents, followed by 6h of drying *in vacuo*. The dried lipid films were suspended by vortexing in sodium phosphate buffer (pH 7.4) and then sonicated intermittently under nitrogen and on ice, with a Heat Systems-Ultrasonics W-225 sonifier until translucent. Centrifugation at 100,000 g for 90 min pelleted titanium probe particles and residual multilamellar vesicles. Analysis by size exclusion chromatography (SEC) confirmed average diameters of ~25 nm (17,34). Glycolipid pool sizes present in the SUV outer leaflets and available for interaction with GLTP were estimated from our previous NMR studies (51, 52).

Preparation of extrusion vesicles. Extrusion vesicles were prepared using 30 nm pore size polycarbonate membranes (58). The appropriate amounts of lipids from stock solutions were thoroughly mixed and dried under nitrogen and then under vacuum for 1 h. The dried lipid mixtures were hydrated in buffer and subjected to fifteen freeze-thaw cycles to ensure uniform distribution of buffer solutes across the bilayers. Rapid freezing was achieved by immersing the lipid suspension in an isopropanol bath cooled by dry ice. During each thawing cycle, the lipid dispersion was raised above 70 °C and vortexed prior to subsequent freezing. The lipid suspension was then extruded with 31 passes through 30 nm polycarbonate membrane using a hand-held mini-extruder (Avanti, Alabaster AL). The resulting vesicles had a narrow size distribution and mean diameters of ~45 nm as measured by SEC using a calibrated Sephacryl S-1000 column (26,39). Glycolipid pool sizes present in the vesicle outer leaflets and available for interaction with GLTP were estimated from Sillence et al. (53).

Supplemental References

54. Mattjus, P., Molotkovsky, J. G., Smaby, J. M., and Brown, R. E. (1999) *Anal. Biochem.* **268**, 297-304
55. Lin, X., Mattjus, P., Pike, H. M., Windebank, A. J., and Brown, R. E. (2000) *J. Biol. Chem.* **275**, 5104-5110
56. Mattjus, P., Pike, H. M., Molotkovsky, J. G., and Brown, R. E. (2000) *Biochemistry* **39**, 1067-1075
57. Huang, C., and Thompson, T. E. (1974) *Meth. Enzymol.* **32**, 485-489
58. MacDonald, R. C., MacDonald R. I., Menco, B. Ph. M., Takesita, K., Subbarao, N. K., and Hu, L. (1991) *Biochim. Biophys. Acta* **1061**, 297-303
59. Santra, M. K., and Panda, D. (2003) *J. Biol. Chem.* **278**, 21336-21343
60. Srivastava, R., Ratheesh, A., Gude, R. K., Rao, K. V. K., Panda, D., and Subrahmanyam, G. (2005) *Biochem. Pharmacol.* **70**, 1048-1055

Figure S1: Tryptophan Topology in GLTP. Space-filling views of the crystal structure of the glycolipid-free form of human GLTP (PDB 1swx). The surface localization of Trp142 and Trp96 (lime-green colored) enables unobstructed access to the aqueous milieu. The lower panel shows how the indole ring of Trp85 is sandwiched between Pro86 and Lys78.

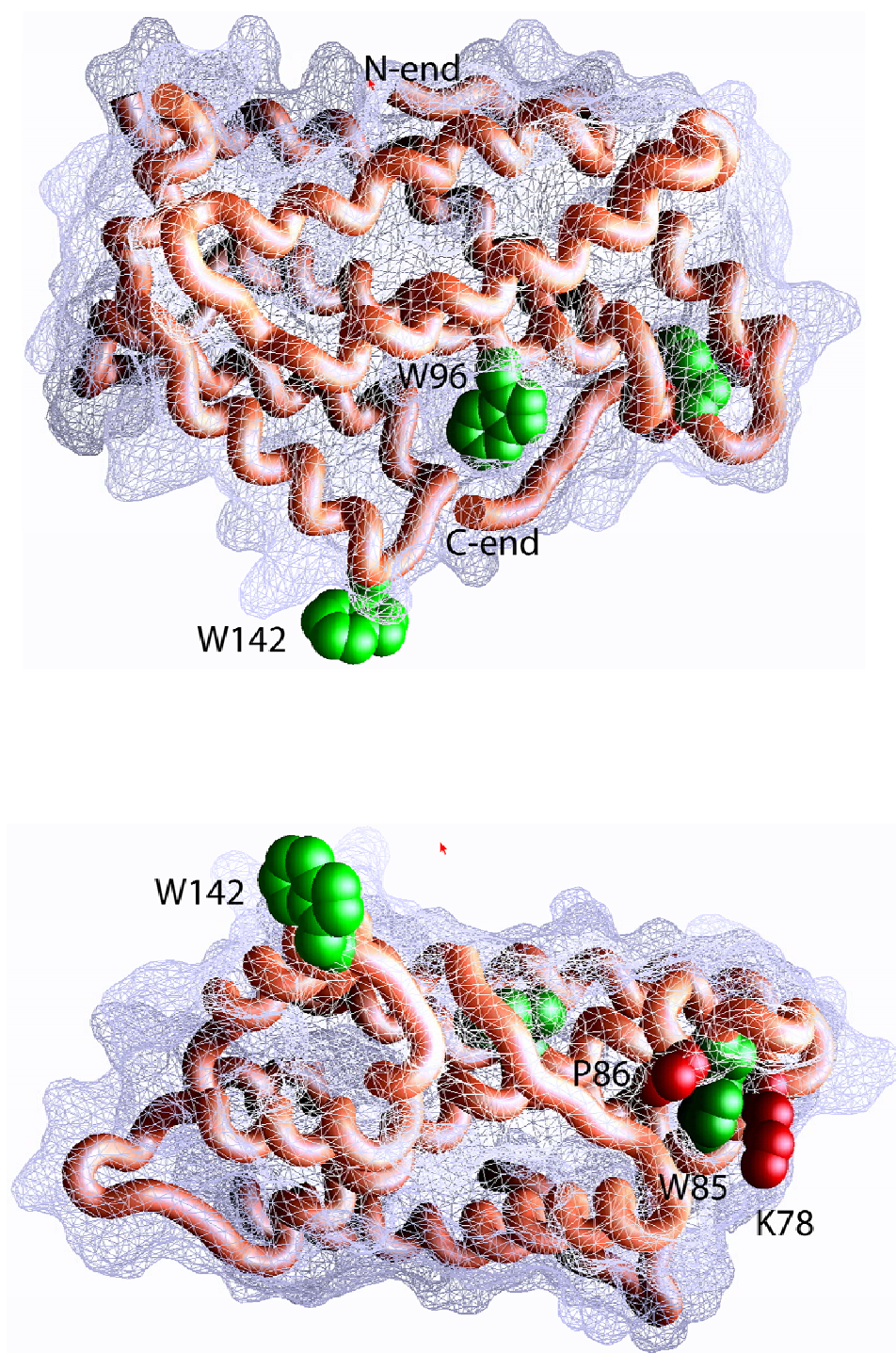


Figure S2: Uptake Kinetics of Different Glycolipids by wtGLTP. Changes in Trp emission of human GLTP (1 μ M) following ethanol-injection of different chain-pure glycolipid species (0.4 μ M). Emission intensity monitored at 353nm while exciting at 295nm. Panels A + B: (■) = 24:0 LacCer; (□) = 24:1 LacCer; (Δ) = 18:0 LacCer; (●) = 16:0 LacCer; (∇) = 18:1 LacCer; (○) = 12:0 LacCer; (\blacktriangle) = 8:0 LacCer. Panels C + D: (■) = 24:0 GalCer; (Δ) = 18:0 GalCer; (\blacktriangle) = 16:0 GalCer; (□) = 12:0 GalCer; (●) = 24:1 GalCer; (■) = 8:0 GalCer; (∇) = 18:1 GalCer; (○) = 18:2 GalCer; (\blacktriangledown) = 8:0 GalCer. Panels D + E: (○) = ganglioside GM1

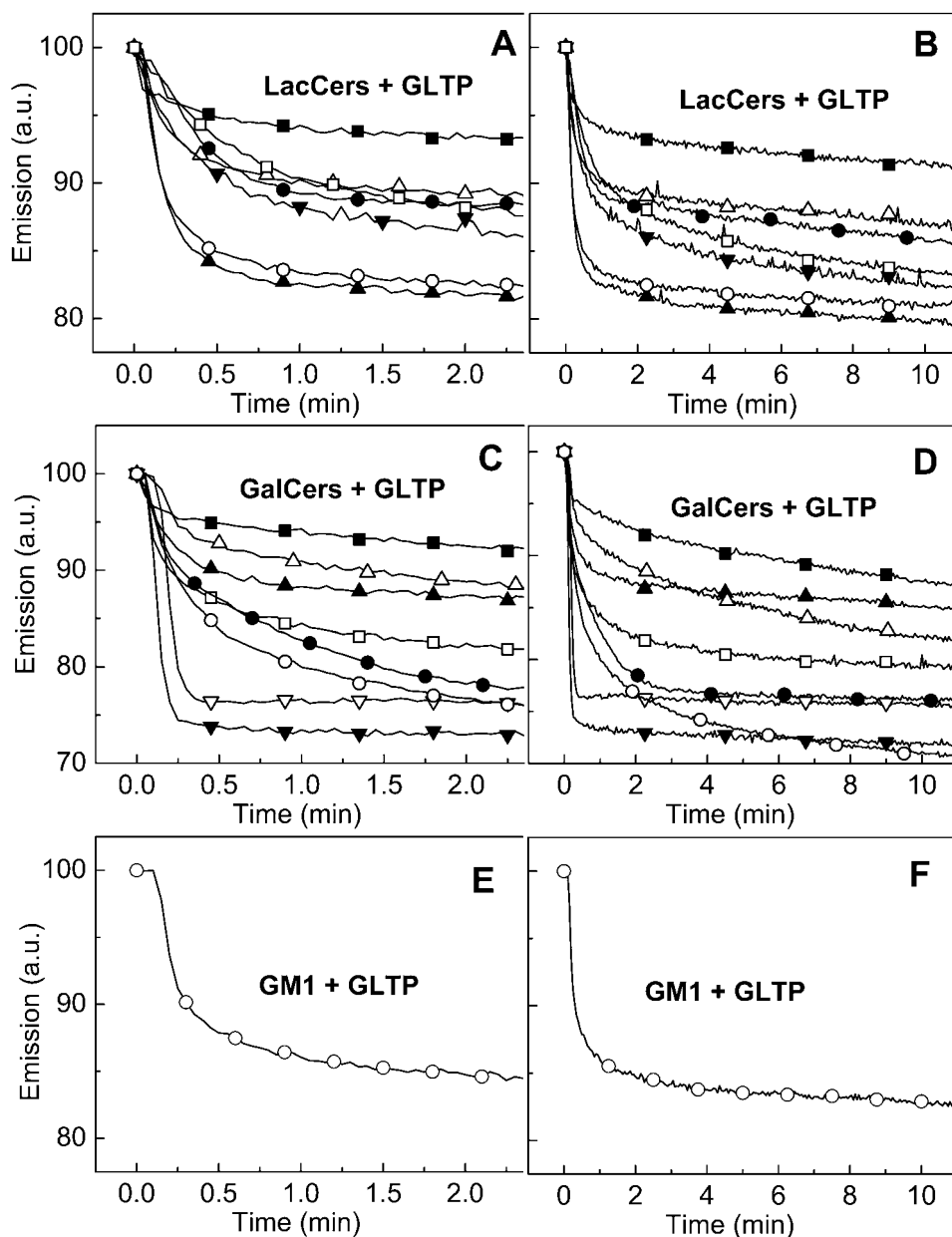


Figure S3: Changes in Trp Emission of W96F GLTP Induced by Incubation with Glycolipid or PC. **A)** 8:0 GalCer; **B)** POPC; Conditions were same as described in Fig. 2 legend. The Trp emission scans correspond to lipid concentrations of 0, 0.08, 0.16, 0.24, 0.32, 0.40, 0.48, 0.56, 0.64, and 0.72 μM with respect to decreasing emission intensity. The Trp emission intensity of W96F GLTP is $\sim 30\%$ of that measured for wtGLTP.

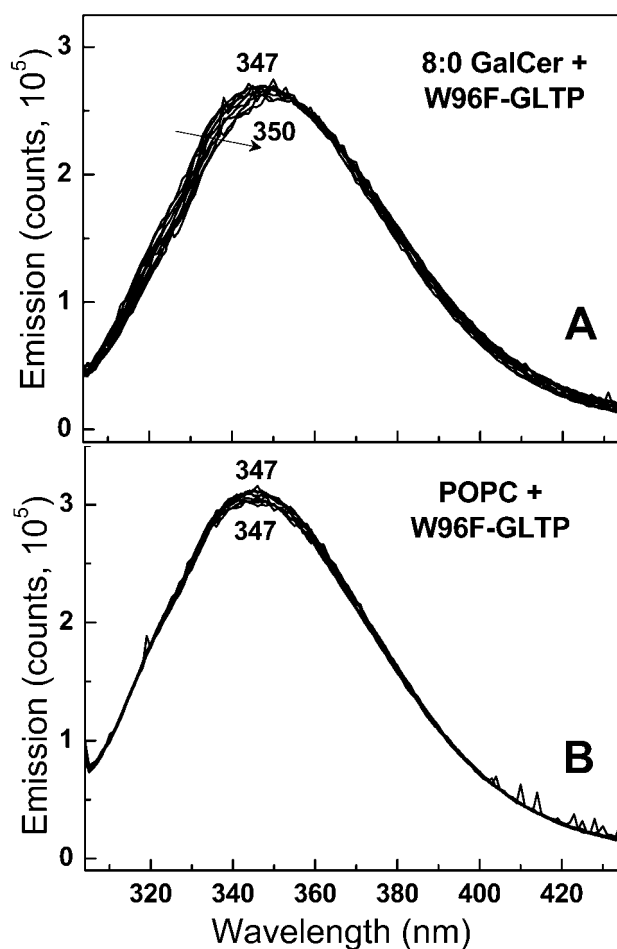


Figure S4: Changes in Trp Emission of wtGLTP by Incubation with Nonglycosylated Sphingolipids or Monochain Glycolipids. **A)** 8:0 ceramide (Cer); **B)** 18:1 sphingomyelin (SM); **C)** glucosyl sphingosine (GlcSph) **D)** hexyl- β -D-glucose; Conditions were same as described in Fig. 2 legend. The Trp emission scans correspond to Cer and SM concentrations of 0, 0.08, 0.16, 0.24, 0.32, 0.40, 0.48, 0.56, 0.64, and 0.72 μ M; to GlcSph concentrations of 0, 2, 4.4, 6, 8, 10, 12, 14, 16, 20, 24, 28, and 30 μ M, and to hexyl glucoside concentrations of 0, 1.9, 9.5, 18.9, 37.8, 56.8, 66.2, 113.5, 151.4, 170.3, and 208.1 μ M with respect to decreasing emission intensity.

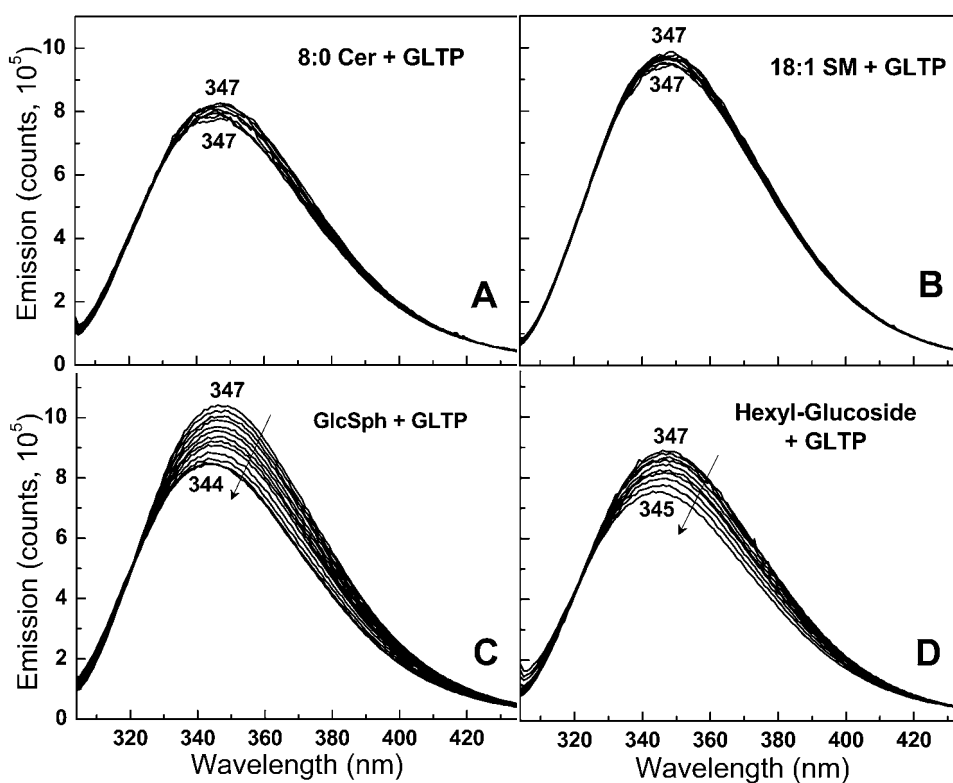


Figure S5: Changes in Trp Emission of wtGLTP by Incubation with Different Chain-Pure GalCers. **A)** 18:1 GalCer; **B)** 24:1 GalCer; **C)** 8:0 GalCer; **D)** 18:2 GalCer; Conditions were same as described in Fig. 2 legend. The resulting Trp emission scans correspond to GalCer concentrations of 0.08, 0.16, 0.24, 0.32, 0.40, 0.48, 0.56, 0.64, 0.72, 0.8, 0.88, 0.96, 1.04, 1.12, and 1.20 μM with respect to decreasing emission intensity.

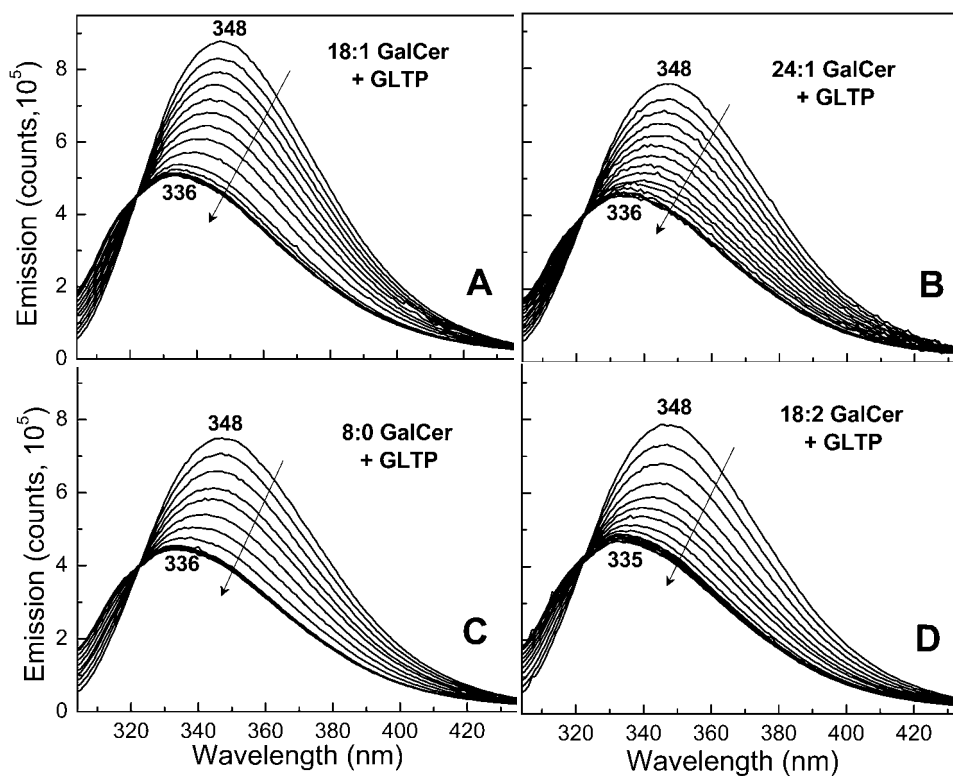


Figure S6: Changes in Trp Emission of wtGLTP by Incubation with Curvature-Stress Free Bilayer Vesicles containing LacCer. **A)** 10 mole% 8:0 LacCer in POPC extrusion vesicles; **B)** 10 mole% 18:1 LacCer in POPC extrusion vesicles. In both cases, the Trp emission scans correspond to extrusion vesicle POPC concentrations of 0, 1.6, 2.4, 3.2, 4.8, 6.4, 8, 9.6, 11.2, 12.8, 14.4, 16, 17.6, 19.2, and 22.4 μM containing 10 mole% LacCer with respect to decreasing emission intensity. Glycolipid pool size in the POPC vesicle outer leaflet and available for interaction with GLTP was estimated from previously reported transbilayer distributions (51-53).

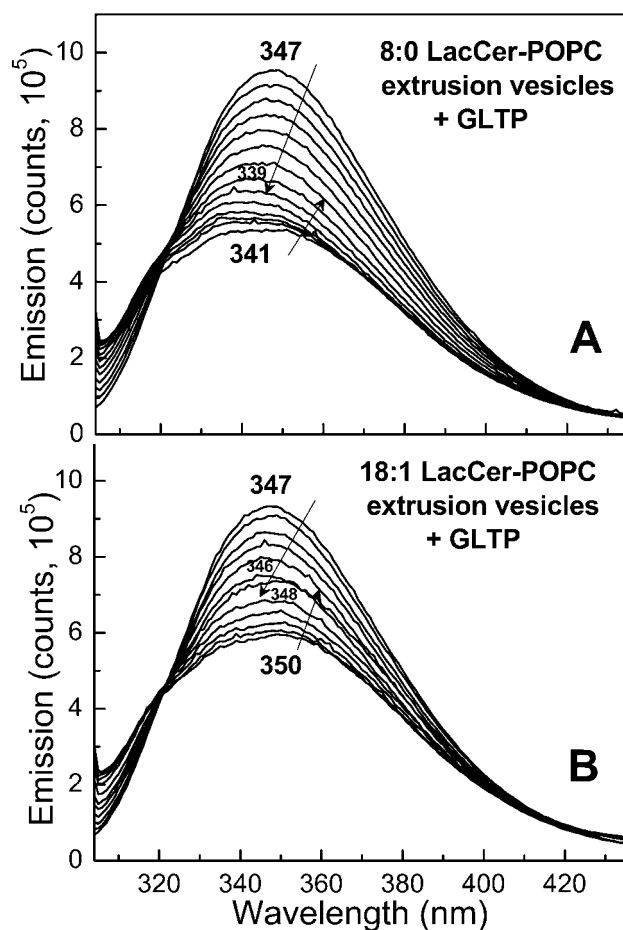


Figure S7: FLPC Size Exclusion Chromatography of 24:1 GalCer/GLTP complex. GLTP was incubated overnight with 24:1 GalCer-POPC SUVs. Uptake of glycolipid was confirmed by measuring the Trp emission maximum wavelength (~336 nm). The 24:1GalCer/GLTP elutes as a monomer based on comparison with the elution positions of protein standards (158, 44, 17, and 1.4 kDa).

